A&A 498, 737–751 (2009)
DOI: 10.1051/0004-6361/200810579

Astronomy & Astrophysics

A lack of close binaries among hot horizontal branch stars in globular clusters⋆

M 80 and NGC 5986

C. Moni Bidin[1], S. Moehler[2], G. Piotto[3], Y. Momany[4], and A. Recio-Blanco[5]

[1] Departamento de Astronomía, Universidad de Concepción, Casilla 160-C, Concepción, Chile
e-mail: cmbidin@astro-udec.cl
[2] European Southern Observatory, Karl-Schwarzschild-Str. 2, 85748 Garching, Germany
[3] Dipartimento di Astronomia, Università di Padova, Vicolo dell'osservatorio 3, 35122 Padova, Italy
[4] INAF - Osservatorio Astronomico di Padova, Vicolo dell'osservatorio 2, 35122 Padova, Italy
[5] Laboratoire Cassiopée UMR 6202, Université de Nice Sophia-Antipolis, CNRS, Observatoire de la Côte d'Azur, France

Received 12 July 2008 / Accepted 27 February 2009

ABSTRACT

Context. Recent investigations have revealed a surprising lack of close binaries among extreme horizontal branch (EHB) stars in the globular cluster NGC 6752, at variance with the analogous sdB field stars. Another puzzling result concerns the derived spectroscopic masses for some EHB stars.
Aims. The present paper extends our study of NGC 6752 to M 80 and NGC 5986, to establish whether the unexpected properties of EHB stars in NGC 6752 are also present in other clusters.
Methods. Twenty-one horizontal branch stars (out of which 5 EHBs) in NGC 5986 and 31 in M 80 (11 EHBs) were observed during four consecutive nights. We measured radial velocity variations and evaluated statistical and systematic errors. Temperatures, gravities, and helium abundances were also measured.
Results. By means of a statistical analysis of the observed radial velocity variations, we detected one EHB close binary candidate per cluster. In M 80, the best estimate of the close binary EHB fraction is $f = 12\%$, and even the lowest estimate of the binary fraction among field sdB stars can be ruled out within a 90% confidence level. Because of the small observed sample, no strong conclusions can be drawn on the close EHB binary fraction for NGC 5986, although our best estimate is rather low ($f = 25\%$).
For the discrepancy in spectroscopic derived masses with theoretical models observed in NGC 6752, our analysis of M 80 EHB stars shows a similar trend. For the first time, we report a clear trend in surface helium abundance with temperature, although the trend for the hottest stars is still unclear.
Conclusions. Our results show that the deficiency of close binaries among EHB stars is now confirmed in two, and possibly three, globular clusters. This feature is therefore not a peculiarity of NGC 6752. Our analysis also proves that the strangely high spectroscopic masses among EHB stars are now confirmed in at least a second cluster. Our results confirm that f could be a function of the age of the sdB star population, but we find that recent models have some problem reproducing all observations.

Key words. stars: horizontal-branch – binaries: close – binaries: spectroscopic – stars: fundamental parameters – globular clusters: individual: M 80 – globular clusters: individual: NGC 5986

1. Introduction

Horizontal branch (HB) stars in Galactic globular clusters are old stars of low initial mass (0.7–0.9 $M_\odot$) which, after the exhaustion of hydrogen in the stellar core and the ascension along the red giant branch, eventually ignited helium core burning (Hoyle & Schwarzschild 1955; Faulkner 1966). The most puzzling feature of these stars is surely the large variety of HB mophologies in globular clusters (see for example Piotto et al. 2002), which is only partly explained by differences in metallicity (the so-called "second parameter problem", Sandage & Wildey 1967; van den Bergh 1967). In this context, the foremost problem is the presence of extreme horizontal branch (EHB) stars at the faint hotter end of HBs ($T_{\rm eff} \geq 20\,000$ K), even in high metallicity clusters like NGC 6388 and NGC 6441 (Rich et al. 1997). EHB stars are identified as hot He-core burning stars with an external envelope too thin to sustain hydrogen shell burning, and after He exhaustion in the core they are expected to evolve directly to the white dwarf cooling sequence without ascending the asymptotic giant branch (AGB manqué stars, Greggio & Renzini 1990). EHB stars have been extensively observed and also studied in the Galactic field, identified as the so-called subdwarf B-type (sdB) stars (Greenstein 1971; Caloi 1972; Heber 1986), although this is a spectroscopic classification without direct link to the stellar evolutionary stage. Given the intrinsic faintness of these objects, they are still spectroscopically poorly observed in globular clusters, and many open problems lack full comprehension (see Moni Bidin et al. 2008b; Catelan 2005, for recent reviews).

One of the most evident features of HB stars is the onset of atmospheric diffusion for temperatures $T_{\rm eff} \geq 11\,000$–$12\,000$ K. This causes changes in their photometric properties (Grundahl et al. 1999), deficiency of helium because of gravitational settling, and strong (solar to super-solar levels) enrichment of heavy

⋆ Based on observations with the ESO Very Large Telescope at Paranal Observatory, Chile (proposal ID 69.D-0682).

metals (Glaspey et al. 1985, NGC6397; Glaspey et al. 1989; Moehler et al. 2000, NGC6752; Behr et al. 1999; Moehler et al. 2003, M13; Behr et al. 2000, M15; Fabbian et al. 2005, NGC1904; Pace et al. 2006, NGC2808). Precise calculations confirmed that diffusion should be at work in the atmospheres of these stars and can account for observed anomalies (Michaud et al. 1983). Michaud et al. (2008) recently confirmed the role of atomic diffusion in the observed abundance anomalies using new stellar evolution models. Spectroscopically determined surface gravities are systematically lower than predictions for stars in this temperature range (Moehler et al. 1995), a problem only partially explained by abundance anomalies (Moehler 2001). Vink & Cassisi (2002) point out that neglecting the presence of stellar wind can cause measured surface gravities to be erroneously low, and an enhanced stellar wind is actually the explanation that Moni Bidin et al. (2007, hereafter M 07) proposed for some bright stars showing erroneously low masses. It is worth noting, however, that optical and UV observations do not support high mass loss rates for field EHB stars in general, with the exception of few relatively luminous objects (Maxted et al. 2001; Lisker et al. 2005). Momany et al. (2002, 2004) found that at temperatures hotter than 23 000 K HB stars deviate again from canonical tracks in the color–magnitude diagram, and they proposed a new onset of diffusion as explanation of this feature. The low helium abundances found by Moehler et al. (2000) and M 07 on some hot stars seem to confirm this hypothesis, but the pattern of abundance with temperature is unclear.

In canonical models, the mass of the He-burning core is approximatively the same for all HB stars, equal to the minimum required for core helium flash ($\approx$0.5 $M_{\odot}$, Schwarzschild & Härm 1962), but the envelope mass decreases for higher temperature. The extremely hot EHB stars retain just a very thin inert hydrogen envelope ($\leq$0.02 $M_{\odot}$, Heber 1986), and must have suffered an extreme mass loss during their evolution. Many single-star evolutionary channels have been invoked to explain EHB star formation in globular clusters, including interactions with a close planet (Soker 1998, see also Silvotti et al. 2007), He mixing driven by internal rotation (Sweigart & Mengel 1979; Sweigart 1997) or by stellar encounters (Suda et al. 2007), dredge-up induced by H-shell instabilities (von Rudloff et al. 1988, but see also Denissenkov & VandenBerg 2003), close encounters with a central, intermediate-mass black hole (Miocchi 2007), and a sub-population of stars with high helium abundance (e.g., D'Antona et al. 2005). The discovery of multiple main sequences in ω Cen (Bedin et al. 2004) and in NGC 2808 (Piotto et al. 2007) reinforced the idea that in some clusters there might be a fraction of stars super-He rich, up to $Y \sim 0.40$ (Norris 2004; Piotto et al. 2005; D'Antona et al. 2005; Lee et al. 2005). Nevertheless binary models, in which sdB stars form through dynamical interactions within binary systems, have been very successful in reproducing observations (Han et al. 2002, 2003, 2007), and are actually the most preferred scenario for field sdB star formation. Indeed, many surveys have shown the existence of a large population of sdB binaries (Ferguson et al. 1984; Allard et al. 1994; Ulla & Thejll 1998; Aznar Cuadrado & Jeffery 2001; Maxted et al. 2001; Williams et al. 2001; Reed & Stiening 2004; Napiwotzki et al. 2004). Among them, close systems with periods shorter than 10 days play a major role (Moran et al. 1999; Saffer et al. 1998; Heber et al. 2002; Morales-Rueda et al. 2003). The close binary fraction among field sdB stars is certainly high but still ill-determined, ranging from 70% (Maxted et al. 2001) to 40–45% (Napiwotzki et al. 2004). In this context, it came as a great surprise that first surveys in globular clusters revealed a lack of close binary systems among the EHB stars (Moni Bidin et al. 2006b, hereafter Paper I). Recently Moni Bidin et al. (2008a) showed that the best estimate of the close binary fraction among EHB stars in NGC 6752 is only $f = 4\%$. On the basis of theoretical and observational results available in the literature, they suggested the presence of a f-age relation. Han (2008) supported this hypothesis with detailed theoretical calculations, showing that the binary scenario naturally predicts a steep decrease of close binary fraction with increasing age of the sdB population. This seems a further success of Han's models, but the general lack of observational data in globular clusters and the uncertainties on the predicted f values (due to uncertainties on model parameters) still requires caution.

Observations of globular clusters other than NGC 6752 are needed to verify that the low fraction of close EHB systems is not a peculiar feature of this cluster. Also other types of binary systems must be included in future searches. In fact, both wide binaries (Reed & Stiening 2004; Morales-Rueda et al. 2006) and systems with very low-mass secondaries (Menzies & Marang 1986) are known to exist among field sdBs (although they are a minor population there) and it has been shown that they can provide an additional channel for the formation of sdB stars.

In this paper we present the results of a binary search in two additional globular clusters, NGC 5986 and M 80. A first analysis of data was presented in Moni Bidin et al. (2006a). Here we refine that preliminary overview with the correction of systematic effects and a detailed error analysis, and we extensively use statistical calculations to better clarify the significance of our results. We also present results about atmospheric parameters and masses for our target stars.

2. Observations and data reduction

We selected 21 HB stars in NGC 5986 and 31 in M 80, spanning a wide range in effective temperature. Targets in M 80 were divided in two fields, named M 80a (17 stars) and M 80b (15 stars), with different slit configurations for multi-object spectroscopy. One star in M 80 (#14327) was accidentally observed in both fields (as star 1a and 12b respectively). The positions of the observed stars along the HB of their parent cluster are shown in Fig. 1, while astrometric and photometric data from Momany et al. (2003) and Momany et al. (2004) are presented in Table 2.

The spectra were collected during four nights of observations (June 11th to 14th, 2002) at the VLT-UT4 telescope equipped with the spectrograph FORS2 in MXU mode. We employed the grism 1400 V with 0.″5– wide slits, and the resulting resolution was 1.2 Å. The 2400 s exposures were always acquired in pairs and subsequently summed, with the exception of one single additional spectrum of NGC 5986 targets during the second night. We finally decided to exclude it from analysis because of its too low , which caused unreliable measurements. The bias, flat, and lamp exposures were acquired during daytime. Just before each pair of exposures, a slit image (without grism) was taken, which was used to correct the spectroscopic data for instrumental effects. The spectral range varied from star to star because of different positions of the slit in the mask, but the H_{β} line was always inside the spectral range.

During each night, we successfully collected at least one pair of medium-resolution spectra for NGC 5986, and the resulting temporal sampling was very good. Unfortunately, because of strong winds from north, observations of M 80 could not be carried out during the entire first night and partially the second one. The starting time of the pairs of exposures is given in Table 1.

During the same run we took two 1350 s exposures of each target with grism 600B, for a resulting resolution of 3 Å, to

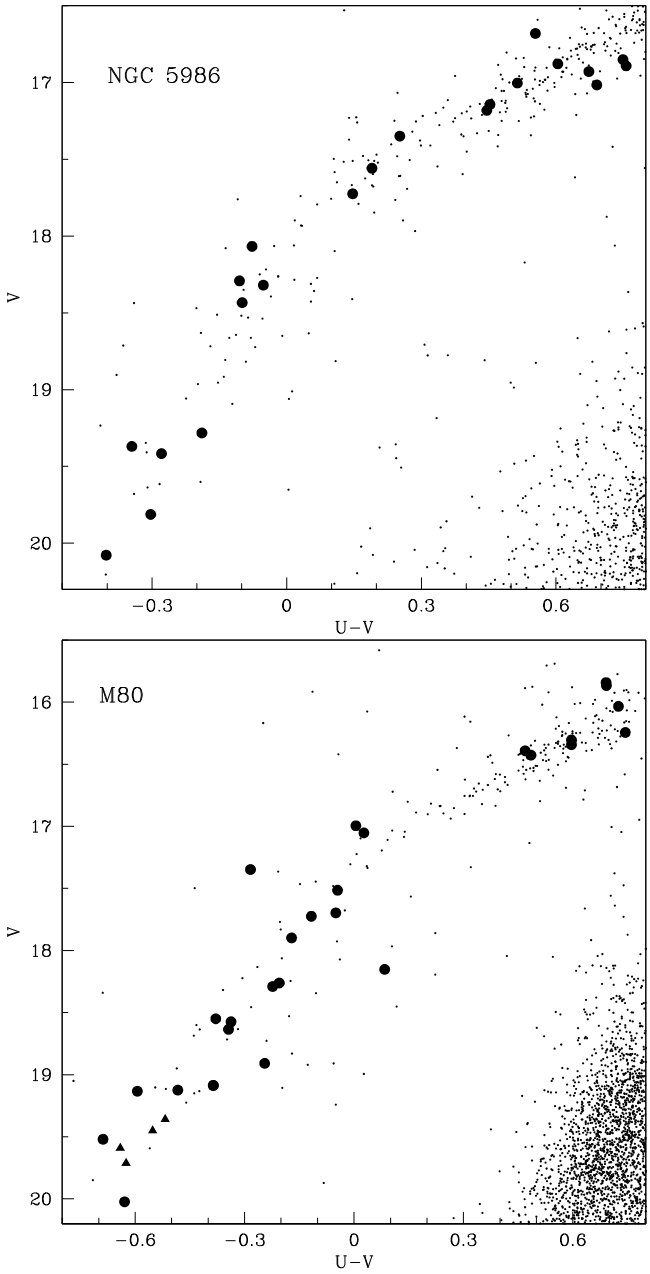

Fig. 1. Color–magnitude diagram of NGC 5986 (*upper panel*) and M 80 (*lower panel*), with targets highlighted. Stars for which we derive anomalously high masses are plotted as full triangles. Photometric data are from Momany et al. (2003) for NGC 5986 and Momany et al. (2004) for M 80.

measure atmospheric parameters. Spectra were trimmed at 3600 Å on the blue side, because of the lack of instrumental response and atmospheric transmission. All Balmer lines from H_β to H10 were always present in these spectra.

Data reduction was performed with standard MIDAS[1] procedures. All slitlets were trimmed from the multi-object frames and reduced independently. The wavelength calibration (wlc) was performed using He and HgCd lamp exposures, fitting a 3rd order polynomial to the dispersion relation for both grisms.

[1] ESO-MIDAS is the acronym for the European Southern Observatory Munich Image Data Analysis System which is developed and maintained by the European Southern Observatory (http://www.eso.org/projects/esomidas/).

Table 1. UT at the start of the first of each pair of exposures.

Field	Night			
	12	13	14	15
NGC 5986	1:18	23:19	3:00	3:00
	3:23			
M 80a	–	6:20	23:27	4:30
			0:53	
M 80b	–	–	4:31	23:32
				0:57

The mean rms of this fit for the medium-resolution spectra was 2.46×10^{-2} Å. All two-dimensional spectra were corrected for curvature along the spatial axis tracing them with a specific MIDAS routine, as described in Moehler & Sweigart (2006), and then extracted with an optimum extraction algorithm (Horne 1986). Sometimes (usually for brighter stars) this procedure failed, producing noisy spectra with irregular continuum, and we opted for a simple sum algorithm in these cases. 1400 V spectra were rebinned to constant steps of 0.25 Å/pix, and continuum-normalized. Most spectra of M 80 stars showed a tiny but clear interstellar emission line in the core of H_β. During data reduction we gave particular attention to the proper removal of this feature, which could spoil the RV variation measurements. 600B spectra were rebinned to a larger constant step (0.4 Å/pix), corrected for atmospheric extinction with the coefficients for La Silla observatory (Tüg 1977), and flux-calibrated. The response curve was obtained separately for each night, through observations of standard stars EG274 and LTT3218 with the flux table of Hamuy et al. (1994). Finally, on 600B spectra we fitted a Gaussian profile to the core of all Balmer lines from H_β to H_9, excluding H_ϵ due to blending with the Ca II H line, and we used the resulting average radial velocity to shift the observed spectra to laboratory wavelengths.

3. Measurements

3.1. Atmospheric parameters and masses

To derive atmospheric parameters by means of Balmer and helium lines fitting, it is important to know whether the stellar atmosphere is affected by diffusion processes. In fact, the profile of lines under study can be influenced by helium depletion and metal enrichment. Moehler et al. (1999, 2000, 2003) showed that strong Fe II lines in the region 4450–4600 Å are detectable even at low resolution when diffusion starts up at about 12 000 K (see for example Fig. 3 in M 07). Therefore, spectra showing evidence of iron lines *or* of being hotter than 14 000 K (as deduced from their position in the color–magnitude diagram) were fit with metal-rich ([M/H] +0.5) model spectra, whereas we adopted metal-poor models ([M/H] = −1.5) for all other stars. In few cases we relied also on higher resolution 1400 V spectra, summed altogether for a higher S/N, in search for evidence of atmospheric diffusion. We kept the helium abundance fixed at solar value ($\log \frac{N_{He}}{N_H} = -1.00$) for cool stars ($T_{eff} \lesssim 11\,000$ K), as the helium lines in their spectra are rather weak. During the fitting we verified that helium lines predicted for these targets agreed with the observed ones.

We computed model atmospheres using ATLAS9 (Kurucz 1993) and used Lemke's version[2] of the LINFOR program

[2] For a description see http://a400.sternwarte.uni-erlangen.de/~ai26/linfit/linfor.html

Table 2. Photometric data of program stars. Columns 1: slit number. Columns 2–6: IDs, coordinates and photometric data from Momany et al. (2003) and Momany et al. (2004).

Slit	ID	RA (J2000) hh:mm:ss	Dec (J2000) °:′:″	V	$(U-V)$
		NGC 5986			
1	17 512	15:46:06.215	−37:50:49.84	18.320	−0.052
2	17 604	15:46:03.177	−37:50:41.41	16.892	0.756
3	17 691	15:46:08.614	−37:50:29.56	19.812	−0.303
4	18 077	15:46:05.939	−37:49:59.20	17.016	0.691
5	18 240	15:46:07.543	−37:49:47.01	16.851	0.749
6	2103	15:46:10.144	−37:48:31.16	17.559	0.190
7	3192	15:46:11.382	−37:48:06.34	18.067	−0.077
8	3560	15:46:12.748	−37:47:58.32	18.434	−0.099
9	4175	15:46:16.056	−37:47:44.62	19.417	−0.279
10	4930	15:46:18.214	−37:47:29.39	17.143	0.453
11	5558	15:46:11.971	−37:47:21.61	17.349	0.252
12	6102	15:46:08.134	−37:47:13.91	17.725	0.147
13	7008	15:46:13.634	−37:46:54.66	16.879	0.604
14	7430	15:46:11.091	−37:46:48.42	17.004	0.514
15	8131	15:46:11.505	−37:46:34.93	19.370	−0.345
16	9049	15:46:04.640	−37:46:21.30	18.292	−0.105
17	9250	15:46:17.684	−37:46:09.79	16.929	0.673
18	10 390	15:46:09.599	−37:45:51.45	16.681	0.554
19	11 215	15:46:11.234	−37:45:30.85	17.182	0.446
20	11 571	15:46:16.004	−37:45:17.74	20.078	−0.402
21	12 099	15:46:09.689	−37:45:05.36	19.282	−0.189
		M 80			
1a	14 327	16:17:11.476	−22:59:23.30	19.086	−0.386
2a	14 786	16:17:10.954	−22:59:06.21	16.304	0.596
3a	14 985	16:17:08.723	−22:58:59.74	18.290	−0.223
4a	15 200	16:17:06.303	−22:58:53.05	18.152	0.084
5a	16 389	16:17:12.046	−22:58:05.56	18.549	−0.379
6a	16 163	16:17:05.336	−22:58:18.14	17.724	−0.117
7a	17 173	16:17:10.234	−22:57:37.98	16.244	0.744
8a	17 114	16:17:07.499	−22:57:42.36	17.515	−0.045
9a	16 707	16:16:56.026	−22:58:04.77	20.023	−0.629
10a	17 737	16:17:03.158	−22:57:21.75	19.359	−0.518
11a	18 516	16:17:07.675	−22:56:45.43	18.635	−0.344
12a	18 110	16:17:00.961	−22:57:07.79	17.053	0.027
13a	18 992	16:17:08.007	−22:56:18.24	16.391	0.469
14a	19 040	16:17:06.095	−22:56:16.68	18.574	−0.337
15a	18 391	16:16:54.498	−22:56:59.78	15.842	0.691
16a	19 191	16:17:03.050	−22:56:07.66	19.124	−0.483
17a	19 127	16:16:55.754	−22:56:16.88	19.450	−0.552
1b	12 304	16:16:58.233	−23:01:19.25	19.590	−0.641
2b	14 201	16:16:57.762	−22:59:37.14	17.898	−0.171
3b	13 787	16:16:59.111	−22:59:53.45	18.261	−0.205
4b	12 663	16:17:01.896	−23:00:48.22	19.133	−0.59
5b	12 767	16:17:03.678	−23:00:40.16	19.712	−0.625
6b	13 839	16:17:03.211	−22:59:48.33	16.342	0.596
7b	14 022	16:17:05.686	−22:59:38.95	18.909	−0.245
8b	14 387	16:17:06.469	−22:59:24.31	17.697	−0.050
9b	12 526	16:17:10.297	−23:00:52.02	19.520	−0.688
10b	13 179	16:17:10.249	−23:00:12.68	17.348	−0.284
11b	15 682	16:17:08.241	−22:58:34.56	16.995	0.005
12b	14 327	16:17:11.476	−22:59:23.30	19.086	−0.386
13b	15 183	16:17:12.947	−22:58:49.48	15.866	0.692
14b	14 813	16:17:14.702	−22:59:02.51	16.427	0.485
15b	15 470	16:17:15.921	−22:58:37.19	16.034	0.725

(developed originally by Holweger, Steffen, and Steenbock at Kiel University) to compute a grid of theoretical spectra that include the Balmer lines H_α to H_{22}, He I (4026 Å, 4388 Å, 4471 Å, 4921 Å), and He II lines (4542 Å and 4686 Å). The grid covered the range 7 000 K $\leq T_{\rm eff} \leq$ 35 000 K, 2.5 $\leq \log g \leq$ 6.0, $-3.0 \leq \log \frac{N_{\rm He}}{N_{\rm H}} \leq -1.0$, at metallicities of [M/H] = −1.5 and +0.5. To establish the best fit to the observed spectra, we used the routines developed by Bergeron et al. (1992) and Saffer et al. (1994), as modified by Napiwotzki et al. (1999), which employ a χ^2 test. The σ necessary for the calculation of χ^2 is estimated from the noise in the continuum regions of the spectra. The fitting program normalizes model *and* observed spectra using the same points for the continuum definition. H_ϵ was excluded to avoid the blended Ca II H line. The errors in each fitting procedure were derived from the χ^2 of the fit itself (see Moehler et al. 1999, for more details), under the assumption that the only error source is the statistical noise. However, Napiwotzki (priv. comm.) noted that the routine underestimates this statistical error by a factor of 2–4. In addition, errors in the normalization of the spectrum, imperfections of flat field/sky background correction, etc. may produce systematic errors, which are not well represented by the error obtained from the fit routine.

For each star, we measured atmospheric parameters in the two 600B spectra separately, and the final results are the weighted mean of the two measurements. Errors were multiplied by $\sqrt{3}$ because the fitting procedure assumes each pixel as independent of the others, but when rebinning we oversampled the spectra by a factor of three with respect to the dispersion. Stars 1a and 12b in M 80, which are actually the same object, were studied as if they were two different targets, so we could compare the results as an indication of their quality. Results are in excellent agreement (see Table 4), despite the target being among the faintest ones, showing that the reported internal errors are probably realistic. The parameters from the two distinct measurements are so similar that we found no need to weight them altogether, hence in our analysis we will simply omit star 12b in order to assure statistical uniformity to our sample. Here, the choice of which star to exclude is quite irrelevant, and we opted to keep star 1a for continuity with RV variation analysis, where the two slitlets are not equivalent because of the better time coverage of field M 80a (see discussion in Sect. 3.2).

Masses were calculated from the previously measured atmospheric parameters, through the equation:

$$\log \frac{M}{M_\odot} = \log \frac{g}{g_\odot} - 4 \cdot \log \frac{T}{T_\odot} - \frac{M_{\rm V} + BC - 4.74}{2.5}, \qquad (1)$$

obtained from basic relations. We adopted the standard values $T_\odot$ = 5777 K and $\log g_\odot$ = 4.4377. The bolometric correction was derived from effective temperature through the empirical calibration of Flower (1996). We adopted an apparent distance modulus $(m-M)_V$ = 15.96 for NGC 5986 and $(m-M)_V$ = 15.56 for M 80 (Harris 1996, February 2003 Web version). Errors on mass estimates were derived from propagation of errors, assuming an uncertainty of 0.1 on photometric quantities (distance modulus, magnitude and BC).

Our results are presented in Table 4. Despite the fact that instruments, observing nights, and measurement procedures were the same as in M 07, the errors are much higher here, This is easily explained by the faintness of the targets in these two clusters with respect to NGC 6752.

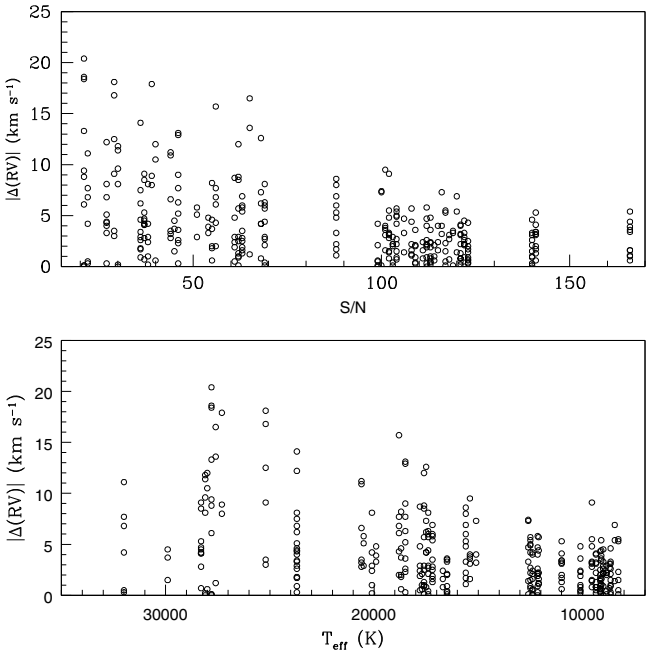

Fig. 2. *Upper panel*: absolute value of measured RV variations of all stars plotted against the spectral S/N. *Lower panel*: same plot but as a function of stellar effective temperature.

3.2. Radial velocity variations

Radial velocity (RV) variations were measured by means of the cross-correlation (CC) technique (Tonry & Davis 1979). The targets are fainter by 1–2 mag with respect to Paper I, and spectra were much noisier despite the longer exposure times. As a consequence, the measurement procedure presents some small difference with respect to previous work, and final errors are higher, especially for hot stars.

We cross-correlated each spectrum with all the others of the same star using the IRAF[3] task *fxcor*. Thus, we measured 10 RV variations for each target in NGC 5986 (5 spectra per star), 6 in M 80a (4 spectra), and only 3 in M 80b (3 spectra). To define the sign of the variation, unnecessary for our goals, the first spectrum in temporal order was always assumed as template. We cross-correlated the single spectra of each pair before summing them, to check that the sum was safe and no RV variation occurred in between exposures. Unfortunately, single spectra of very hot stars were often of too low S/N for a reliable CC, and they were summed *bona fide*.

RV variation measurements focused on H_β line with full wings. Based on our experience, the CC of such a wide line fails to give the correct shift of the spectra if restricted to line cores, and results tend to lower values if the adopted interval is too narrow. On the other hand, on larger intervals, the results converge to a fixed value, but the line wings provide progressively less information and more noise. We performed tests on artificially shifted spectra, looking for the best compromise, and eventually we adopted the interval 4830–4890 Å in our CC. The CC function roughly resembles the line profile, and in our case it took the shape of a Gaussian core with wide wings. We performed a Gaussian fit of the central peak to determine its center. For hotter stars, the low S/N (see Fig. 2) required the application of a Fourier filter (Brault & White 1971). The resulting CC function lost its strong irregularities and was easier to fit, but we always verified that RV variation after filtering did not differ from what could be (sometimes with difficulties) deduced fitting the unfiltered CC function.

We always tried to confirm the measured RV variation cross-correlating weaker spectral lines. On hotter stars this proved fruitless, because too low S/N caused unreliable (often even impossible) measurements. Results agreed with H_β, but within so large errors that the confirmation was useless. On cooler stars we obtained very good CCs but they just confirmed measurements on H_β, without additional information. Hence, we will not analyze results obtained with lines other than H_β.

3.2.1. Corrections on radial velocity variations

RV variations were corrected as in Paper I. The reader is referred to Paper I for an extensive discussion. In brief, we first used the [O I] 5577 Å sky emission line as a zero-point to correct the spectral shift with respect to the arc lamp observations. The position of the forbidden line was determined with a Gaussian fit. After this, we corrected RV variations caused by different positions of the stars within the slits, using the slit images secured before each pair of exposures.

The corrections to be applied clearly correlate with the spatial Y coordinates on the CCD (see Figs. 5 and 7 of Paper I). In both steps we preferred to obtain the final corrections from a least-square fit as a function of Y, to reduce the additional noise added to the final results. The correction procedure on field M 80b was straightforward. On NGC5986 and M 80a we sometimes found mismatches between the derived corrections and RV variations to be corrected, in a way very similar to Fig. 7 of Paper I (middle panel). This indicates movements of the mask inside its frame between the slit and science images, as already discussed in Paper I. On the other hand, we found negligible indication of rotation of the masks (i.e. different slope between corrections and RV variations when plotted against spatial coordinate). It was recently found[4] that the central wavelength for FORS2 data varies with the temperature at the telescope focus. This fact also could explain the observed shifts of spectra on CCD, but we found no clear correlation between them and focus temperature differences as obtained from frame headers. Moreover, no shift was observed among spectra in field M 80a, as among many frames studied by Paper I, despite the fact that temperature changes occurred. We must conclude that in some cases we observe small rigid shifts of spectra on CCD not caused by different centering of stars in the slits, that can be corrected because they affect simultaneously all the spectra in the same frame (see Paper I, for details). They cannot be explained by variations of the temperature at telescope focus alone, and movements of the mask within its frame must play a role, although the two causes could act together and sum their effects.

3.2.2. Errors on radial velocity variations

The analysis of RV variations in search of binary systems requires an accurate error analysis, because the crucial point is to tell if variations are consistent with random measurement errors or are an indication of binarity. As discussed later (Sect. 5),

[3] IRAF is distributed by the National Optical Astronomy Observatories, which are operated by the Association of Universities for Research in Astronomy, Inc., under cooperative agreement with the National Science Foundation.

[4] see http://www.eso.org/observing/dfo/quality/FORS2/reports/HEALTH/trend_report_LSS_lambda_c_T_HC.html

Table 3. "Extraction and fit" errors (in km s^{-1}) for each field and different S/N range.

S/N	Field		
	NGC 5986	M 80a	M 80b
≥80	1.2	1.2	1.0
40–80	2.1	3.0	3.0
≤40	6.3	5.0	5.4

varying estimated errors by 10% can noticeably change the probability of the datum, up to a factor of two.

We estimated the error associated to each RV variation as the quadratic sum of all relevant sources. The wavelength calibration error was deduced from the rms of the calibration procedure, and it was directly calculated by the calibration routine. Its exact value changed from spectrum to spectrum, but the differences were negligible in the final quadratic sum, therefore we kept this contribution fixed to the mean value of 1.5 km s^{-1}. This is in good agreement with the error estimated in Paper I for the same instrumentation, obtained analyzing calibrated lamp images. The error introduced by the correction of systematic effects (Sect. 3.2.1) were estimated as in Paper I, from the uncertainty in the sky line peak position, and the scatter of residuals with respect to the least-square solutions used for the corrections. We did not find any relevant difference with respect to Paper I, and we adopted a fixed $\sigma_{\rm sky}$ = 1.5 km s^{-1} for the first correction uncertainty and $\sigma_{\rm corr}$ = 1.1 km s^{-1} for the second one. Wavelength calibration and sky-line correction errors were considered twice in the quadratic sum, because in each RV variation two spectra were involved.

Additional uncertainties were introduced by the choice of the parameters determining the CC function fit and of the spectrum extraction, because different extractions caused noise-induced differences in the line profile. They were estimated re-extracting spectra in slightly different ways and re-fitting CC functions for all hot stars and a sample of cooler ones. The dispersion of the differences between the measurements was assumed as an estimate of the error. This parameter is very sensitive to spectral noise, and we grouped stars in each cluster in three ranges of S/N. The resulting errors are given in Table 3. In Fig. 2 we plot the absolute value of RV variations for all stars, as a function of their S/N and temperature, excluding the three binary candidates discussed in Sect. 5 (two EHB and a cool target). The trend of decreasing dispersion with increasing S/N is clear.

3.3. Absolute radial velocities

Absolute RVs were measured on 1400 V spectra by means of CC with synthetic spectra of appropriate temperature and gravity drawn from the library of Munari et al. (2005). We verified that the template metallicity had negligible effects on the results. Each measurement was corrected to make the [O I] 5577 Å sky line coincide with its laboratory wavelength, then the weighted mean was computed to derive the final absolute RV. The error resulting from the weighting procedure was unrealistically small, and for the final error we adopted the dispersion of the single measurements. Results are shown in Table 4.

Within errors, all stars show an absolute RV compatible with parent cluster. We can conclude that NGC 5986 targets are most likely cluster members. For M 80 stars we can just state that RV does not disprove cluster membership. In fact, because of the very low cluster RV (8.2 km s^{-1}, Harris 1996, February 2003 Web version), we cannot distinguish members from foreground Galactic disk stars, which are expected to contaminate the field at such low Galactic latitudes (b = 19.°5, Harris 1996, February 2003 Web version). Indeed, we have reasons to suspect that some cool stars are main sequence foreground objects (as discussed in Sect. 4), but their absolute RVs do not noticeably differ from the cluster value. The RV of star #14327 in M 80 was measured separately in both fields, but results are identical in value and error.

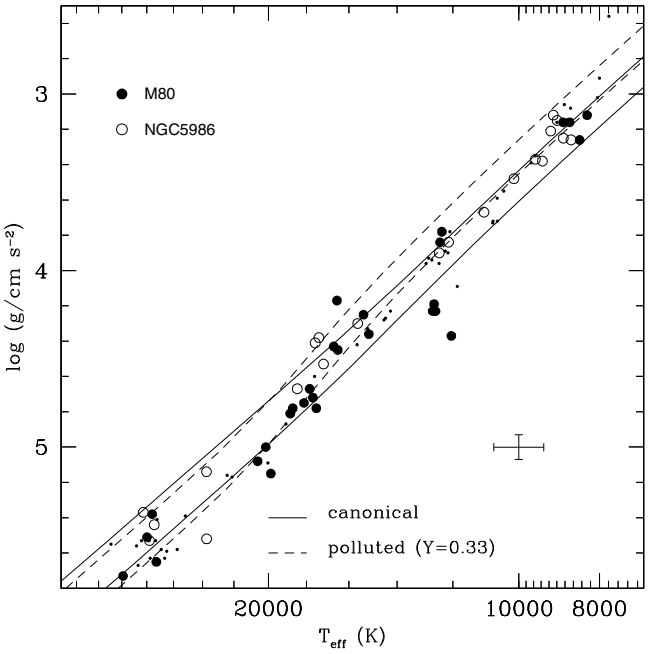

Fig. 3. $T_{\rm eff}$–log(g) plot of observed stars. (full points: NGC 5986, open points: M 80). Errorbars on single stars are omitted for clarity, but the errorbar drawn in *lower right* corresponds to typical values $\frac{\sigma(T_{\rm eff})}{T_{\rm eff}}$ = 0.03, σ(log(g)) = 0.07 dex. Small points indicate results on NGC 6752 from M 07. Zero-age (ZAHB) and terminal-age (TAHB) horizontal branch theoretical tracks are also indicated, for [M/H] = –1.5 and canonical models (Y = 0.24) and polluted ones (Y = 0.33) (see Moehler et al. 2003, for details).

4. Results on atmospheric parameters and masses

The 600B spectrum of star #16707 in M 80 fell between the two FORS2 chips, and we could not measure its atmospheric parameters. Its 1400 V spectra were well inside the second chip, because of the offset between the two grisms in the spatial direction, and RV variation measurements proceeded normally. We deduced its effective temperature from its color, for the only purpose of its classification in our search for binarity (Sect. 6).

Our results on effective temperatures and gravities are plotted in Fig. 3, where we compare the position of our target stars with theoretical models. The zero-age (ZAHB) and terminal-age (TAHB) HB theoretical tracks for [M/H] = −1.5 from Moehler et al. (2003) are indicated, both for canonical models of normal He-content (Y = 0.24) and polluted ones with enhanced helium abundance (Y = 0.33). The ZAHB and TAHB define the region where models spend 99% of their HB lifetime.

In Fig. 3 four M 80 stars at $T_{\rm eff}$ ≈ 12 000 K stand out for their too high gravities. The fitting procedure outlined in Sect. 3.1 was usually problematic for these targets, although both 600B and 1400 V spectra were of good quality and no problems were encountered during reduction. Their spectra show a high

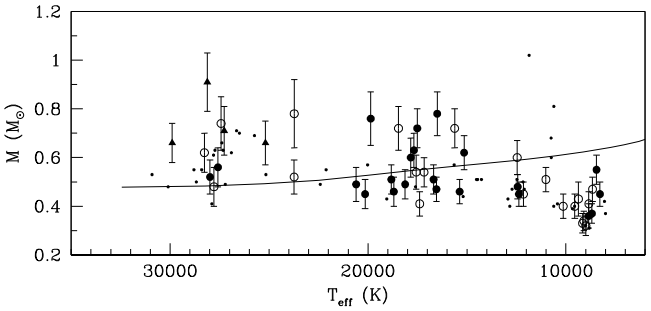

Fig. 4. Calculated masses of program stars as function of effective temperature. Symbols are as in Fig. 3. M 80 stars which show anomalous masses are plotted as full triangles. Errorbars on temperatures are omitted for clarity. Also the theoretical HB (Moehler et al. 2002) is indicated.

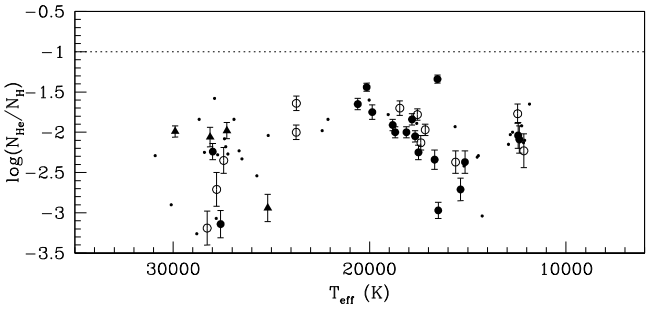

Fig. 5. Measured surface helium abundance for program stars. Symbols are as in Fig. 3. Errors in temperature are omitted for clarity. The dotted line indicates the solar value.

quantity of strong metallic lines, but the fit with super-solar metallicity models is not convincingly better and, on the contrary, for two of these targets it was too poor to permit parameter determination. For this reason, the tabulated and plotted results throughout this paper refer to fits with parent cluster metallicity models, although they should not be the more appropriate. Their derived masses are very high compared to canonical values (2.5–5 $M_\odot$), and temperatures are completely inconsistent with their color: these stars can be found in Fig. 1 at the reddest end of the HB ($U - V \approx 0.7$), far from other HB stars with the same temperature and redder than the coolest "normal" HB stars with $T_{\rm eff}$ = 8500 K. All these results point to a mismatch between their spectra and theoretical models, and we suspect these objects are foreground main sequence stars. This hypothesis is further corroborated by their metal-rich spectra, that would be very surprising for HB cluster members much redder than the Grundahl jump. Both temperatures and masses are roughly consistent with this explanation, but they might not be reliable. In particular, masses could be overestimated by Eq. (1), due to a wrong distance modulus. For one of these four stars we detect some RV variability on 1400 V spectra, as analyzed in Sect. 6.

Our results agree fairly well with theoretical expectations, and, within errors, the global behavior of all the points in Fig. 3 is to follow the canonical track, although the presence of some He-enhanced stars can not be excluded. One may note that the tendency toward lower gravities in the range $T_{\rm eff}$ = 12 000–17 000 K, that moves the points closer to the polluted models than the canonical ones, could also be explained by stellar winds unaccounted for by the model atmospheres. As discussed in M 07, this hypothesis better explains the too low masses observed for many targets in this temperature range (see Sect. 4.1), because evolutionary effects or enhanced helium abundance would cause both lower gravity and higher luminosity, and the calculated mass would agree with expectations.

4.1. Masses

Our results on masses resemble what found on NGC 6752 and discussed in M 07, and are plotted in Fig. 4. In brief, masses are systematically lower than theoretical prediction for stars cooler than 10 000 K and in the range $T_{\rm eff}$ = 12 000–15 000 K, while they agree with models for $T_{\rm eff}$ = 15 000–23 000 K. Beyond $T_{\rm eff}$ = 23 000 K some stars are "normal", while others show an anomalously high mass.

For temperatures below 10 000 K masses are too low in both clusters, as found in NGC 6752, despite the fact that the gravities in Fig. 3 agree better with the canonical tracks. We conclude that the problem of low masses in this temperature range cannot be fully explained only by erroneously low gravities. Between 15 000 and 23 000 K, masses fairly scatter around the theoretical track. As already discussed in M 07, this favors evolutionary effects or enhanced helium as explanation of the low gravities measured for many stars among 15 000 and 17 000 K, and it argues against the hypothesis of an enhanced stellar wind (unaccounted for in the models used for parameter measurements), that would cause underestimated masses.

Above 23 000 K we cannot draw strong conclusions as done in M 07, because of the small number of stars and higher errors. In particular, in NGC 5986 we observed only five targets, and they are too scattered in the color–magnitude diagram to try to divide them in different families. On the other hand, in M 80 we can confirm what we found in NGC 6752. In fact, we overestimate masses with respect to theoretical predictions for four out of six stars, and all of them are systematically redder and slightly fainter than the two for which masses are "normal". These stars are indicated as full triangles in all figures. Hence, the strange dichotomy extensively discussed in M 07 is present also in this cluster. We remind the reader that this behavior of masses is not a consequence of photometric data, because stars with higher derived masses are fainter, while a lower luminosity alone would imply a lower calculated mass. Hence, these stars appear both photometrically *and* spectroscopically distinct with respect to stars showing normal masses. The explanation for this behavior is still obscure. Higher masses are expected for EHB stars formed through a merging event of two He white dwarfs (Han et al. 2002), but predictions are still much lower than measured values. We believe the too high masses are not physical, but just an effect of a mismatch between real stars and adopted model atmospheres. The same model atmospheres give good mass estimates for some stars and bad for others, suggesting that the actual stellar atmospheres are intrinsically different between the two groups of EHB stars.

4.2. Helium abundance

The helium abundance was kept fixed to solar value for stars cooler than about 11 000 K, which showed no evidence of diffusion (see Sect. 3.1). Results for hotter stars are shown in Fig. 5. The plot reveals a clear trend with effective temperature followed by all stars in the three clusters, although it passed unnoticed by M 07 because masked by the lack of stars between 15 000 and 20 000 K (see their Fig. 8). The helium abundance turns to sub-solar values at 12 000 K, possibly reaching a minimum at 15 000–16 000 K, then rises again steeply and

continuously up to about 22 000 K. Finally helium abundance decreases again, but this transition region is undersampled. For stars hotter than 25 000 K the helium abundances scatter between $-3 \leq \log \frac{N_{\rm He}}{N_{\rm H}} \leq -2$. They possibly follow a double-peaked distribution rather than a wide single one, but this can be only guessed from the data. The same general trend can be seen also in Moehler et al. (2003, their Fig. 5) and, concerning the first decrease between 12 000 and 15 000 K, in Behr (2003) and Fabbian et al. (2005), while it was probably hidden by larger errors in Moehler et al. (2000). Helium depletion caused by diffusion is usually coupled with metal overabundances and, interestingly enough, even the iron abundances measured by Pace et al. (2006, their Fig. 4) in NGC 2808 follow the same trend observed here, reaching a maximum at about 15 000 K and then decreasing at higher temperatures.

The observed behavior of helium surface abundances with temperature does not come unexpected. On the contrary, it confirms theoretical expectations based on our current understanding of diffusion processes in the atmospheres of HB stars. Early results of Glaspey et al. (1989) and later detailed studies by many authors (see Sect. 1) showed that surface abundances abruptly change at $T_{\rm eff} \approx 11\,000$ K. The most common interpretation of the observed phenomena relies on the disappearance of the He I convection zone at this effective temperature, that would be responsible for the gravitational settling of helium, with its consequent depletion in a thin radiative layer between the surface and the region of He II ionization. Within this picture, this layer becomes thinner for increasing temperatures, because the second He ionization region moves outward (Sweigart 2000), and moreover mass-loss (which contrasts diffusion, Michaud & Charland 1986) increases (Vink & Cassisi 2002). As a net result, the efficiency of diffusion would be expected to decrease with increasing temperature, as also suggested by the photometric properties of stars which, after the Grundahl jump, progressively reduce the discrepancies with standard models. This is exactly what we are observing between 15 000 and 23 000 K. Unfortunately, this scenario has recently been ruled out by the latest theoretical models, which show that diffusion affects layers much deeper than the depth of the He I convection zone (Michaud et al. 2008, see their Fig. 5). Actually, the models that best reproduce the observed trend of surface metal abundances assume that the outer regions down to $^{\rm M}M_{\odot} = 10^{-7}$ are completely mixed by turbulence, well below the He I ionization zone (Sweigart, priv. comm.). In other words, turbulence from this convective layer is not able to inhibit levitation in Michaud's models. Michaud et al. (2008) tentatively attribute the onset of levitation at ≈11 000 K to an abrupt change in stellar rotational velocity as observationally confirmed (e.g. Recio-Blanco et al. 2002; Behr 2003), but the issue is currently under debate.

Momany et al. (2002) proposed a new onset of diffusion at about 23 000 K, causing the photometrical anomaly known as "Momany Jump". Unfortunately the behavior of helium abundance among hotter stars is hard to decipher. Both our present results and previous ones on NGC 6752
(Moni Bidin et al. 2007; Moehler et al. 2000) show that helium is depleted between a factor of 10 and 100 for these stars, confirming that diffusion is active at these temperatures, but with a scatter that is much larger than observational errors. Stars with the same temperature and different helium depletion seem to coexist. Even evolutionary effects cannot be ruled out, as helium surface abundance could be a time-dependent result of competing processes (Michaud et al. 1983). As already noted in M 07, the helium abundances of EHB stars are not related with anomalous masses discussed in 4.1. For example, stars #12663 and #19127 are strongly depleted in helium ($\log(N({\rm He})/N({\rm H})) \approx -3$), but the mass is "normal" for the first and too high for the second one.

The comparison of our results with Fig. 1 of O'Toole (2008) can be very instructive. In that plot the author summarizes current knowledge about the trend of helium abundance with temperature for field sdB stars, gathering the data from many extensive surveys (Edelmann et al. 2003; Lisker et al. 2005; Ströer et al. 2005; Hirsch et al. 2008). The aim of O'Toole (2008) is to analyze the two families of field EHB stars discovered by Edelmann et al. (2003), one being a factor of ten more depleted in helium than the other. Field stars cooler than 20 000 K are undersampled, but they clearly do not follow the trend observed by us in three globular clusters. On the contrary, the helium abundances in the figure of O'Toole seem to decrease monotonically from 12 000 K to at least 23 000 K. We have no explanation for this difference, but we think it deserves further investigation.

At a first glance, results for globular cluster EHB stars agree fairly well with those for field EHB stars, with a possible small decrease of helium abundance between 20 000 and 23 000 K, and hotter stars being scattered between $\log(\frac{N_{\rm He}}{N_{\rm H}}) = -1.8$ and -3.2. Hence, quite surprisingly, we would not be observing any evidence of a second, more depleted family of stars. These are only about 15% of field EHBs in the studied temperature range, and it might be possible to explain their absence in our sample by their relative scarcity alone. Nevertheless, we would statistically expect about 4 such stars in our sample. If these He-poorer objects were stars with no core He-burning, as proposed by O'Toole (2008), there would be no clear reason for their absence in globular clusters. However, at a further inspection an alternative interpretation is possible. In fact, comparing the diagrams one could suspect that an offset is present for EHB stars, with our abundances being higher by about 0.5 dex. For example, our stars with $T_{\rm eff} = 20\,000$ K cluster at about $\log \frac{N_{\rm He}}{N_{\rm H}} = -1.5$, while in Fig. 1 of O'Toole (2008) they are at about −2. Lowering our abundances by 0.5 dex in Fig. 5, the bulk of EHB stars would lie between $\log \frac{N_{\rm He}}{N_{\rm H}} = -2$ and -3, while five stars would be much more depleted, at about $\log \frac{N_{\rm He}}{N_{\rm H}} = -3.7$. In this case, the helium abundance of both the main population and He-depleted stars, and even the number ratio of the two families of EHB stars, would excellently agree with results among sdB stars. However, arguing for the presence of this offset is quite speculative, because stars cooler than 20 000 K show no evidence of it. The procedure adopted here to measure helium abundance is very standard for sdB studies, and we share the fitting routine with almost all field surveys. Even the model atmospheres are often the same (e.g. Edelmann et al. 2006), and no offset has ever been observed. To verify an *intrisic* higher helium abundance for our cluster EHB stars would require a more extensive sample. As a conclusion, the presence of a helium-poorer EHB population in globular clusters, analogous to what is observed among field stars, must currently remain an open issue.

Comparing our results with theoretical expectations is difficult, because the effects of diffusion processes still lack a full comprehension. Recent calculations of Michaud et al. (2008) well reproduce observed surface abundances, but their trend with effective temperature (that is our observational result) is still unexplored. Moreover, a detailed model prediction cannot neglect the counter-acting effects of stellar wind, which are still poorly known. In fact, they are suspected to play an important role, because helium abundances among sdB stars are much too high to be accounted for by diffusion models (Michaud et al. 1989), and weak stellar winds can explain the discrepancy

Table 4. Results for program stars. Columns 1: ID as in Table 2. Columns 2–7: absolute radial velocity, fundamental parameters (effective temperature, surface gravity, helium abundance and mass) and maximum radial velocity variation.

ID	$V_{\rm rad}$	$T_{\rm eff}$	$\log g$	$\log(\frac{N_{\rm He}}{N_{\rm H}})$	M	$\Delta({\rm RV})_{\rm max}$
	km s^{-1}	K			$M_\odot$	km s^{-1}
			NGC 5986			
17 512	75 ± 6	17 400 ± 400	4.38 ± 0.07	−2.13 ± 0.09	0.41 ± 0.05	8.1 ± 3.7
17 604	–	8850 ± 150	3.25 ± 0.07	−1.00 ± 0.00	0.41 ± 0.05	–
17 691	94 ± 6	23 700 ± 1200	5.52 ± 0.12	−1.64 ± 0.09	0.78 ± 0.14	12.2 ± 8.1
18 077	81 ± 6	9350 ± 130	3.38 ± 0.14	−1.00 ± 0.00	0.43 ± 0.07	4.1 ± 3.5
18 240	76 ± 6	8650 ± 90	3.26 ± 0.05	−1.00 ± 0.00	0.47 ± 0.05	4.6 ± 3.5
2103	87 ± 5	12 150 ± 150	3.84 ± 0.05	−2.23 ± 0.21	0.45 ± 0.05	5.8 ± 3.2
3192	80 ± 5	17 600 ± 400	4.41 ± 0.07	−1.78 ± 0.07	0.54 ± 0.07	12.0 ± 4.1
3560	92 ± 7	17 200 ± 300	4.53 ± 0.05	−1.97 ± 0.07	0.54 ± 0.06	6.9 ± 3.7
4175	93 ± 11	27 400 ± 800	5.44 ± 0.10	−2.35 ± 0.16	0.74 ± 0.11	26.9 ± 7.0
4930	98 ± 5	10 100 ± 160	3.48 ± 0.07	−1.00 ± 0.00	0.40 ± 0.05	4.8 ± 3.1
5558	84 ± 6	12 500 ± 150	3.90 ± 0.05	−1.77 ± 0.12	0.60 ± 0.07	5.7 ± 3.3
6102	93 ± 9	15 600 ± 300	4.30 ± 0.05	−2.37 ± 0.14	0.72 ± 0.08	8.6 ± 5.6
7008	81 ± 5	9000 ± 160	3.15 ± 0.08	−1.00 ± 0.00	0.32 ± 0.04	4.5 ± 3.2
7430	90 ± 7	9550 ± 140	3.37 ± 0.07	−1.00 ± 0.00	0.40 ± 0.05	9.1 ± 3.4
8131	89 ± 7	28 300 ± 700	5.37 ± 0.08	−3.19 ± 0.21	0.62 ± 0.08	9.1 ± 6.0
9049	92 ± 6	18 500 ± 500	4.67 ± 0.07	−1.70 ± 0.09	0.72 ± 0.09	13.1 ± 6.2
9250	91 ± 6	9150 ± 140	3.21 ± 0.08	−1.00 ± 0.00	0.33 ± 0.04	4.3 ± 3.3
10 390	89 ± 7	9100 ± 130	3.12 ± 0.07	−1.00 ± 0.00	0.34 ± 0.04	5.4 ± 3.2
11 215	91 ± 7	11 000 ± 110	3.67 ± 0.03	−1.00 ± 0.00	0.51 ± 0.05	5.3 ± 3.3
11 571	102 ± 10	27 800 ± 900	5.53 ± 0.12	−2.71 ± 0.21	0.48 ± 0.08	20.4 ± 7.2
12 099	103 ± 11	23 700 ± 800	5.14 ± 0.08	−2.00 ± 0.09	0.52 ± 0.07	14.1 ± 5.9
			M 80			
14 327	15 ± 7	20 100 ± 700	5.00 ± 0.08	−1.44 ± 0.05	0.45 ± 0.06	8.1 ± 5.8
14 786	6 ± 4	8280 ± 50	3.12 ± 0.02	−1.00 ± 0.00	0.45 ± 0.05	5.5 ± 3.3
14 985	6 ± 9	17 500 ± 400	4.78 ± 0.05	−2.25 ± 0.09	0.72 ± 0.08	12.6 ± 4.6
15 200	12 ± 6	17 800 ± 500	4.67 ± 0.07	−1.84 ± 0.07	0.60 ± 0.08	8.7 ± 4.3
16 389	3 ± 9	18 100 ± 400	4.75 ± 0.05	−2.00 ± 0.07	0.49 ± 0.06	23.1 ± 4.6
16 163	5 ± 5	15 400 ± 200	4.25 ± 0.05	−2.71 ± 0.14	0.46 ± 0.05	9.5 ± 4.6
17 173	10 ± 13	12 700 ± 300	4.23 ± 0.12	−1.00 ± 0.00	2.40 ± 0.39	26.4 ± 3.3
17 114	8 ± 4	16 500 ± 300	4.45 ± 0.05	−2.97 ± 0.10	0.78 ± 0.09	3.6 ± 3.3
16 707	4 ± 7	–	–	–	–	11.1 ± 6.8
17 737	1 ± 5	28 100 ± 700	5.69 ± 0.08	−2.06 ± 0.12	0.91 ± 0.12	11.8 ± 6.1
18 516	10 ± 5	18 700 ± 500	4.78 ± 0.07	−2.00 ± 0.07	0.46 ± 0.06	8.2 ± 4.2
18 110	10 ± 4	12 400 ± 150	3.84 ± 0.03	−2.04 ± 0.16	0.48 ± 0.05	4.2 ± 3.1
18 992	7 ± 4	8850 ± 180	3.16 ± 0.08	−1.00 ± 0.00	0.36 ± 0.05	2.9 ± 3.1
19 040	15 ± 5	18 800 ± 400	4.81 ± 0.05	−1.91 ± 0.07	0.51 ± 0.06	15.7 ± 6.2
18 391	12 ± 3	12 100 ± 200	4.37 ± 0.07	−1.00 ± 0.00	5.13 ± 0.64	5.7 ± 3.2
19 191	13 ± 9	20 600 ± 600	5.08 ± 0.07	−1.65 ± 0.07	0.49 ± 0.07	11.2 ± 5.1
19 127	13 ± 11	25 200 ± 700	5.51 ± 0.08	−2.94 ± 0.17	0.66 ± 0.09	18.1 ± 7.7
12 304	7 ± 6	27 300 ± 600	5.65 ± 0.08	−1.98 ± 0.10	0.71 ± 0.10	17.9 ± 7.3
14 201	16 ± 5	16 700 ± 400	4.43 ± 0.05	−2.34 ± 0.12	0.51 ± 0.06	2.4 ± 3.2
13 787	1 ± 4	17 700 ± 300	4.72 ± 0.05	−2.05 ± 0.07	0.63 ± 0.07	2.1 ± 3.2
12 663	19 ± 5	27 600 ± 700	5.38 ± 0.08	−3.14 ± 0.17	0.56 ± 0.08	16.5 ± 6.0
12 767	20 ± 9	29 900 ± 500	5.73 ± 0.05	−1.99 ± 0.07	0.66 ± 0.08	4.5 ± 4.7
13 839	−4 ± 11	8450 ± 40	3.26 ± 0.02	−1.00 ± 0.00	0.55 ± 0.06	6.9 ± 3.2
14 022	−11 ± 9	19 900 ± 800	5.15 ± 0.08	−1.75 ± 0.09	0.76 ± 0.11	4.8 ± 4.9
14 387	1 ± 8	15 100 ± 300	4.36 ± 0.05	−2.37 ± 0.14	0.62 ± 0.07	7.3 ± 3.2
12 526	6 ± 15	28 000 ± 700	5.51 ± 0.08	−2.24 ± 0.10	0.52 ± 0.07	12.0 ± 6.3
13 179	15 ± 7	16 500 ± 300	4.17 ± 0.05	−1.34 ± 0.05	0.47 ± 0.05	3.5 ± 3.1
15 682	14 ± 10	12 400 ± 200	3.78 ± 0.05	−2.09 ± 0.17	0.45 ± 0.05	4.0 ± 3.1
14 327	15 ± 7	20 500 ± 500	5.06 ± 0.07	−1.42 ± 0.05	0.49 ± 0.06	5.8 ± 4.5
15 183	0 ± 15	12 600 ± 400	4.19 ± 0.12	−1.00 ± 0.00	3.09 ± 0.06	7.4 ± 3.2
14 813	15 ± 9	8700 ± 100	3.16 ± 0.05	−1.00 ± 0.00	0.37 ± 0.04	3.1 ± 3.1
15 470	8 ± 6	12 600 ± 300	4.23 ± 0.12	−1.00 ± 0.00	2.95 ± 0.48	4.7 ± 3.2

(Fontaine & Chayer 1997; Unglaub & Bues 1998). The combination of diffusion and stellar wind could also produce time-dependent surface abundances, although on a relatively short time scale, that could affect the results by introducing an intrinsic star-to-star scatter. A detailed comparison of our results with field sdB stars would also require a precise knowledge of the effects of metallicity. In fact, field sdBs should on average be younger and more metal-rich than our sample. Unglaub (2008) showed that strong coupled stellar winds, involving H and He in addition to accelerated metals, are prevented for metal-poor EHB stars. The effects of this result on the helium surface abundance is not stated by the author, but it could be an important clue to interpret the differences between our results and the plot of O'Toole (2008).

5. Radial velocity variations

The arc lamp spectra for star #17604 in NGC 5986 were damaged by lines of hot pixels, resulting in a wavelength calibration without the precision required by our aims. The target is very cool, adding little information to our search for binaries focused on EHB stars, and we considered safer to exclude it from analysis.

Our radial velocity results are summarized in Fig. 6, where we plot the maximum variation for each star. Variations are taken always positive, the sign just being a consequence of the arbitrary definition of "template" and "object" spectrum. We indicate the 3σ interval with thinner errorbars.

We detect RV variations above 3σ for one of the four cool targets suspected to be foreground main sequence stars in M 80 (Sect. 4), indicating it could be a spectroscopic binary. We did not find evidence for a companion in our spectra, although at our low resolution its features could be easily hidden by the lines of the brighter primary. We found that all weak lines, in particular Fe lines and the MgIb triplet, follow H_β in its RV variations. Therefore, the companion could be a compact object or a low-mass main sequence star. No other cool stars shows any variability within our errors. Hence, no close binary is detected among them, in agreement with recent results from a large sample of cool HB stars in NGC 6752 (104 HB stars with $T_{\rm eff} \leq 20\,000$ K, Moni Bidin et al. 2008a).

Star #14327 shows no noticeable RV variation in both field M 80a and M 80b. We also checked that no variation occurs between its spectra in the two fields. Nevertheless, it is the only star observed seven times, and in order to avoid in the statistical analysis one star with different temporal sampling with respect to all the others, we will simply exclude results from slit 12b, thus considering this star as a normal target observed in field M 80a only. The choice of the slit to exclude is dictated by the better temporal sampling of M 80a field.

Among the EHB stars we detect one interesting close binary candidate for each cluster, namely star #4175 in NGC 5986 (maximum variation 26.9 ± 7.0 km s^{-1}) and #16389 in M 80 (maximum variation 23.1 ± 4.6 km s^{-1}). Variations for these targets are small compared to those observed on typical sdB close binaries (see for example Maxted et al. 2001; Morales-Rueda et al. 2003), but so are the errors. In particular, CC errors for these measurements are very small compared with stars with similar S/N. In our experience, this could be an indirect indication that the variation is real and not due to noise-induced distortion of the CC function. Some stars show variations at the edge of the 3σ interval, although not formally outside it, and we want to verify if other candidates could hide among them. We performed statistical calculations on all EHB targets to translate these considerations into numbers. Results are summarized in Table 5. The star IDs and the maximum observed RV variations are indicated in Cols. 1 and 2, respectively. In Col. 3 the maximum RV variation is given in units of σ. To estimate the significance of variations near the 3σ threshold, in Col. 4 we calculated the probability that a variation greater or equal to $\frac{\Delta(\mathrm{RV})_{\max}}{\sigma}$ occurs among the measurements, assuming a normal distribution of errors. From basic statistical relations, we have:

$$p\left(\frac{\Delta(\mathrm{RV})_{\max}}{\sigma}\right) = 1 - \left[\mathrm{erf}\left(\frac{\Delta(\mathrm{RV})_{\max}}{\sqrt{2}\sigma}\right)\right]^n, \quad (2)$$

where n is the number of independent measurements (10 in NGC 5986, 6 in M 80a, and 3 in M 80b), and

$$\mathrm{erf}(x) = \frac{2}{\sqrt{\pi}} \int_0^x \mathrm{e}^{-t^2}\,\mathrm{d}t. \quad (3)$$

Finally, we calculated the fraction of typical sdB close binaries with random phase and inclination angle, a 0.5 $M_\odot$ companion, and period $P \leq 10$ days, that in our survey would show a RV variation *not* greater than the maximum observed. This is an estimate of how likely the small observed variations can really indicate a close binary. Results are tabulated in Col. 5. We included in the analysis one cool target (#14985 in M 80) with RV variations near 3σ, marked with an asterisk in Table 5.

The numbers in Table 5 help to clarify the situation. First, the two stars that show variations greater than 3σ are confirmed to be good candidates, in view of the negligible probability of the observed datum being a random variation. Their variations are indeed small, but not enough to rule out binarity: about two out of three typical sdB binaries would show higher variations in our observations but, for example, this fraction would decrease if we assume a lower mass companion.

For all other EHB targets, except for field M 80b because of poor temporal sampling, the variations are unlikely to be caused by binarity because of low probabilities in Col. 5, although it cannot be excluded on the basis of this datum alone. The numbers in Col. 4 are more conclusive, and they do not allow us to claim the detection of any other binary candidate. In some cases the probability of the datum is low, but not negligible. One doubtful exception could be star #12663 in M 80, but the probability of its observed RV variation being random is still at least one order of magnitude higher than for the two proposed candidates. Moreover, it is important to notice that this probability is extremely sensitive to the adopted error value. We calculated that probabilities lower than 4% in Col. 4 would double if errors were 10% larger. Despite our efforts, we feel that our error estimates are unlikely to be more precise than this value. Therefore these low probabilities should be considered accurate only to within a factor of two.

In summary, the numbers support the hypothesis of binarity for only one star per cluster, the only ones which show variations greater than 3σ. This indicates that requiring a variation greater than 3σ for the detection of a binary system is a good choice, and in the statistical analysis we will assume this value as detection threshold.

The only other EHB close binary discovered to date in a globular cluster (Moni Bidin et al. 2008a) shows a MgIb triplet anomalously strong for stars at its temperature (Moni Bidin et al. 2007), indicative of a cool main sequence companion. We inspected the sum of all the V 1400 spectra, but we never found evidence for this feature in any EHB target. Therefore, the companions of our binary candidates are most likely compact objects (as white dwarfs), or very low-mass main sequence stars. In fact,

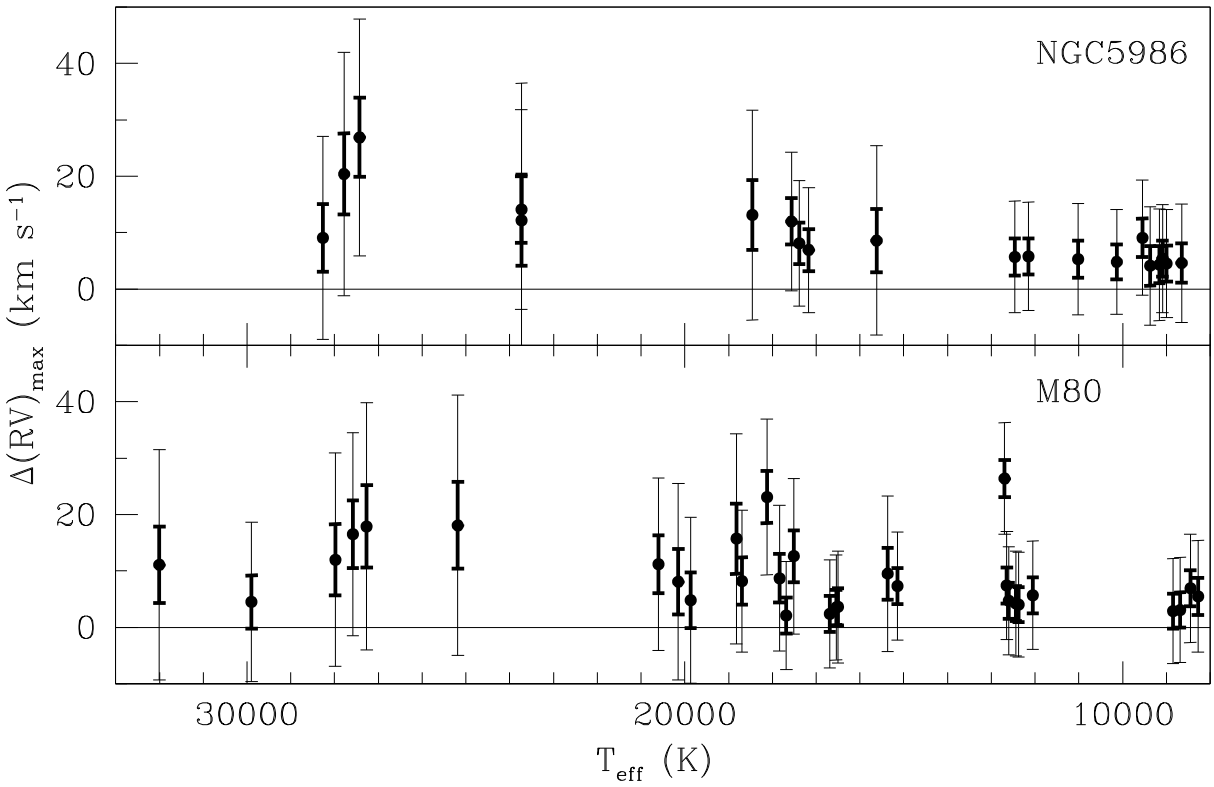

Fig. 6. Maximum radial velocity variation observed for program stars. Thin errorbar indicates the 3σ interval.

Table 5. Statistical analysis of RV variations for our target EHB stars.

ID	$\Delta(RV)_{max}$ (km s^{-1})	$\frac{\Delta(RV)_{max}}{\sigma}$	$p\left(\frac{\Delta(RV)_{max}}{\sigma}\right)$ (%)	$p\,(\leq \Delta(RV)_{max})$ (%)
NGC 5986				
17 691	12.2	1.51	73.6	11.9
4175	26.9	3.84	0.15	28.3
8131	9.1	1.52	73.6	8.3
11 571	20.4	2.83	4.0	21.2
12 099	14.1	2.39	13.4	14.1
M 80				
14 327	8.1	1.40	60.4	11.9
14 985*	12.6	2.74	3.0	19.5
16 389	23.1	5.02	2.4×10^{-6}	35.1
16 707	11.1	1.63	44.6	35.1
17 737	11.8	1.93	26.7	18.2
19 191	11.2	2.20	14.2	17.2
19 127	18.1	2.35	10.0	28.0
12 304	17.9	2.45	3.5	51.0
12 663	16.5	2.75	1.5	48.3
12 767	4.5	0.96	65.2	17.5
14 022	4.8	0.98	65.2	18.5
12 526	12.0	1.90	14.4	38.6

we have no indication about the period, and very low-mass companions in close nearly edge-on orbits can cause large RV variations (see for example the NY Vir system, Vučković et al. 2007). Thus, a low-mass main sequence companion is plausible.

6. EHB close binary fraction

In the statistical analysis of our results we will assume the detection of two EHB close binaries, one per cluster, as discussed in Sect. 5. The candidate in M 80 is slightly cooler than the typical temperature boundary for EHB stars ($T_{\rm eff} \geq 20\,000$ K). The distinction is more than just a conventional definition, because it approximately sets the transition between classical HB stars with envelopes sufficiently massive to sustain the hydrogen-burning shell, and EHB stars, which do not have this second energy source. The post-HB evolution is also very different, as depicted in Sect. 1. It can also be noted from Fig. 1 that at approximately 20 000 K there is an underpopulated region in the HB of both clusters, and the binary in M 80 is brighter than this gap (at $V \approx 18.7$), indicating that it is indeed cooler than typical EHB stars. Despite these arguments, we consider that excluding the candidate from statistical analysis on the basis of its temperature alone would be quite artificial. In fact, field surveys usually focus on hotter stars, excluding targets with lower temperatures (see for example Maxted et al. 2001), but they are sometimes included (Ulla & Thejll 1998), and binary systems are detected among them (Aznar Cuadrado & Jeffery 2001). Population synthesis models also indicate that sdBs as cool as 15 000–16 000 K can be formed by interactions within binary systems (Han et al. 2003). Moreover, relatively massive (0.75 $M_{\odot}$) EHB stars, or with a relatively massive envelope ($\geq$0.01 $M_{\odot}$), move to temperatures lower than 20 000 K during the first stages of post-EHB evolution (Han et al. 2002). Hence, the candidate could even be an evolving object. Its exclusion would strengthen the results in favor of a lack of close systems.

In the previous section we found that some hot stars show marginally significant RV variations. We emphasize that the following analysis does not depend on whether we consider them as candidates or not. In fact, once the detection threshold is fixed,

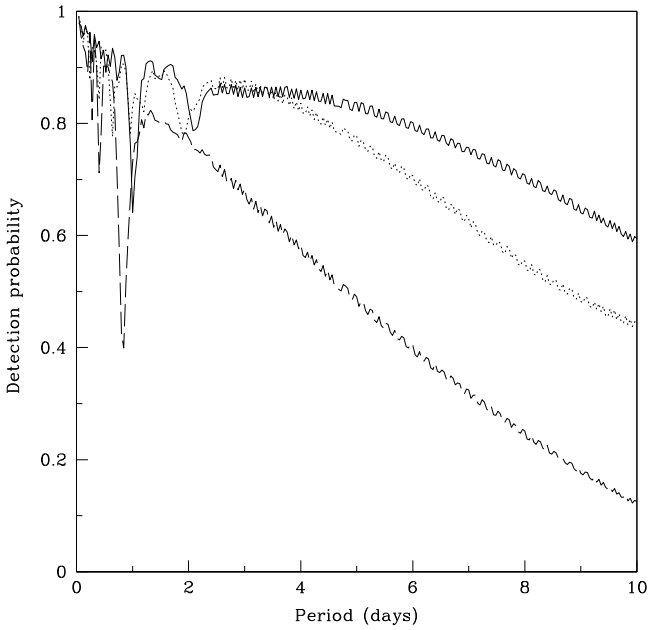

Fig. 7. Probability of binary detection in our survey, as a function of binary period. *solid line*: NGC 5986. *dotted line*: field M 80a. *dashed line*: field M 80b. The calculation assumes a companion of 0.5 $M_\odot$ in circular orbit.

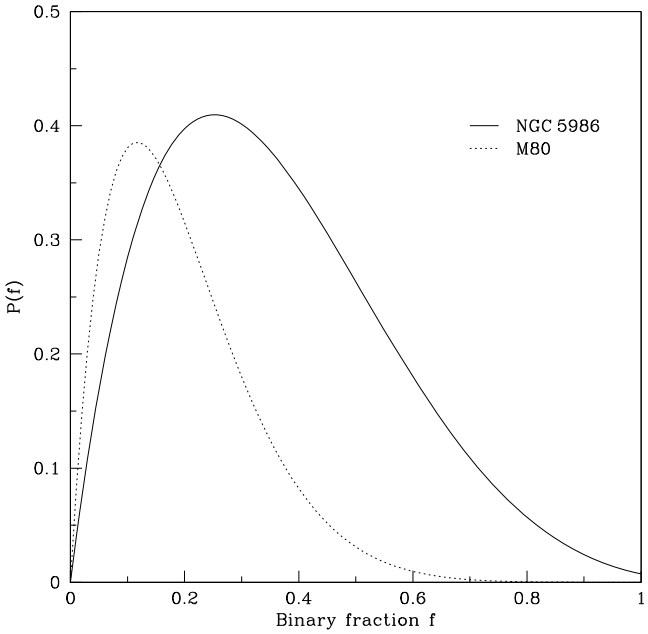

Fig. 8. Curves of probability for the close binary fraction f, as calculated from our results. *solid line*: NGC 5986 (binaries with periods $P \leq 10$ days). *dotted line*: M 80 (periods $P \leq 5$ days).

the only input is the number of stars with variations above and below it, and the routines automatically consider undetected systems (because of unfavorable temporal sampling or low inclination angles) as part of the calculations.

The close binary detection probability of our survey was calculated as in Paper I. In brief, 2500 typical sdB binaries (with a 0.5 $M_\odot$ companion in circular orbit, as assumed for example by Maxted et al. 2001; Morales-Rueda et al. 2006) were simulated for each value of period P, evenly distributed in the phase-sin i space (where i is the inclination of orbit with respect to the line of sight). Then we calculated the fraction of these synthetic systems that would have been detected in our observations, i.e. showing RV variation greater than the detection threshold. We fixed the threshold at the 3σ value, because we found (Sect. 5) that variations lower than this value are not sufficiently significant. We adopted $3\sigma = 20$ km s^{-1} for NGC 5986 and 18 km s^{-1} for M 80, which are average values for our program stars and well represent the typical accuracy of measurements. Results are plotted in Fig. 7. The detection probability for NGC 5986 is high, as a consequence of the good temporal sampling. On the contrary, the lack of data in the first two nights for M 80, due to bad weather, strongly damaged the efficiency of the survey, mainly in the field M 80b. We will limit our analysis to periods $P \leq 5$ days on this cluster, as done by Moni Bidin et al. (2008a) for similar reasons. This limitation is not too severe, because our main aim is the comparison with results on field sdB stars. The exact shape of their period distribution is still unknown, but is suspected to be strongly peaked at $P = 1$ day, and binaries with $P \geq 5$ days represent only the tail of the distribution (see for example Fig. 2 of Morales-Rueda et al. 2006).

The probability of detecting N_B binaries out of a sample of N targets is:

$$p = \frac{N!}{(N - N_B)!N_B!}(\bar{d}f)^{N_B}(1 - \bar{d}f)^{N-N_B}, \quad (4)$$

where f is the binary fraction and $\bar{d}$ is the probability of detection weighted with the period distribution. For M 80 we used the mean of the detection probability of the two fields, weighted with the number of EHB targets observed in each. The shape of the period distribution affects the results only marginally, as already demonstrated by Paper I and Moni Bidin et al. (2008a). A Gaussian distribution in $\log P$ centered on $\log P = 0$ days, as proposed by Maxted et al. (2001) and Napiwotzki et al. (2004), does not change p(f) by more than 0.01–0.03 with respect to the flat distribution we assumed here. We used the relation (4) as a function of f to calculate the probability p(f), given our observational results of one detection out of five targets in NGC 5986 and one out of eleven in M 80. As stated before, we must limit our analysis to periods $P \leq 5$ days on M 80. The results of our calculations are plotted in Fig. 8. The curves are far from being Gaussian-shaped, hence we cannot simply deduce a best estimate with an associated error. Nevertheless, from their analysis we can draw important conclusions.

6.1. NGC 5986

In NGC 5986 the most probable value of $f_{P\leq 10\ \mathrm{days}}$ is 25%, as indicated by the peak of the curve in Fig. 8. This must be considered the best estimate for the EHB close binary fraction in this cluster. Nevertheless, the small number of targets implies a very wide curve, so that no value of f can be safely excluded. A very high binary fraction as proposed by Maxted et al. (2001) for field stars is not probable, but cannot be completely ruled out ($p(f = 0.7) = 10.9\%$). The probability of our best estimate is $p(f = 0.25) = 41\%$, which does not noticeably differ from $p(f = 0.4)$. Hence, a binary fraction as high as the lowest determination among field sdB stars is not preferred, but it is perfectly reasonable. There is no improvement in limiting to periods shorter than 5 days, because the width of the probability curve is dictated by small number statistic and not by the sensitiveness of the survey. We conclude that our data do not give strong constraints on the EHB close binary fraction for this cluster, and they agree both with the unexpected low estimates found in NGC 6752 (Moni Bidin et al. 2006b, 2008a), *and* with the

lowest determinations for field sdBs (Napiwotzki et al. 2004). They tend to exclude high binary fractions as proposed by Maxted et al. (2001) for field sdBs. Given the most probable value, the results hint that the real fraction could be relatively low.

6.2. M 80

Stronger results can be obtained on M 80. The best estimate is $f_{P\leq5\ \mathrm{days}} = 12\%$, very low compared to any determination among field stars. High values are ruled out ($p(f = 0.7) = 0.2\%$). Results well agree with the extremely low fraction found by Moni Bidin et al. (2008a) in NGC 6752 ($p(f = 0.04) = 25\%$), much more than the lowest values for field sdBs, which are very improbable for this cluster ($p(f = 0.4) = 8.2\%$). Within a 90% confidence level, f is lower than 38%.

In summary, although our results are not as strong as previous ones on NGC 6752, we find that *also in M 80 EHB close binary systems are lacking*, at variance with what is observed among field sdBs. The binary fraction is not very well constrained, but values observed among field samples are very unlikely, while results agree well with the tiny 4% found in NGC 6752 (Moni Bidin et al. 2008a). M 80 is the second globular cluster for which a lack of EHB close systems is found, and this indicates that it should not be a peculiarity of NGC 6752. Preliminary results by Moni Bidin et al. (2008b) suggest that some clusters could be different, but the early stage of their analysis and their small number statistics strongly call for further investigation. In Sect. 1 we discussed the models for the still unclear sdB star formation mechanisms. In light of these results, any successful model must take into account the significant difference between stars inside and outside globular clusters.

6.3. Comparison with Han (2008) results

As mentioned in Sect. 1, Han (2008) confirmed with theoretical calculations that the binary scenario naturally implies a f-age relation, as proposed by Moni Bidin et al. (2008a). In brief, the model assumes that dynamical interactions in binary systems are responsible for sdB star formation, but the efficiency of the various channels varies with the age of sdB progenitors, leading to a decreasing fraction of *close* binaries with increasing mean age of the population.

The general conclusion of our work, that f is low also in a second globular cluster and possibly in a third one, is a fair confirmation of Han's model. The fraction predicted in NGC 6752 by his preferred set of parameters (2%) fairly agrees with observational results of Moni Bidin et al. (2008a). Unfortunately, a direct comparison for the two new globular clusters is complicated by the large uncertainties in both model predictions and empirical determinations. Therefore, the analysis cannot rely on exact values, but on the general behavior of the results.

The best estimates of f in the three clusters so far surveyed are all smaller than those found for the field sdB stars, but too different from each other if compared to Han's prediction. The lowest observed fraction is for NGC 6752 and the highest is for NGC 5986. The order is correct, because NGC 6752 is the oldest cluster while NGC 5986 is the youngest one (De Angeli et al. 2005), but age difference is too small, about 2 Gyr, compared with the modeled f-age relation.

The parameter set preferred by Han creates an f-age relation that fairly agrees with observations of NGC 6752, but its predictions are not easily compatible with our new results: the model implies a nearly constant $f = 2\%$ for populations older than 10 Gyr. Despite the uncertainties in our study, it is clear that this low value is improbable in both NGC 5986 (6% probability) and M 80 (14%, see Fig. 8). The combined probability, i.e. the probability that $f \approx 2\%$ in both cluster is negligible, according to our observations. This tends to exclude the f-age relation derived by this model. Other models studied by Han (2008, see his Fig. 3), with different sets of input parameters, predict higher close binary fractions and a steeper relation with age, thus solving the outlined contradictions, but their high expected f are incompatible with measurements in NGC 6752, the more robust of the observed results.

From this analysis we conclude that, despite the good general agreement (close EHB binaries are predicted and observed to be a minor population), models and observations still lack a good agreement on the details, although observational constraints are still not strong enough to be conclusive. Maybe the discrepancies could be mitigated by a refined set of model parameters, or some other effect (like dynamical interactions in dense environments) could be invoked to slightly change f from cluster to cluster.

It is important to note that the present comparison strongly relies on our results on M 80, which are the most precise, and the low temperature of the binary candidate in this cluster leaves space for doubts on the feasibility of the comparison itself. In fact, Han (2008) did not apply any temperature cut, but his f-age relation was obtained taking into account a GK selection effect[5], and models corrected to consider this bias tend to exclude sdBs as cool as our target (Han et al. 2003). Anyway, the system in M 80 should not be a EHB+MS wide binary (Sect. 5) as the systems selected against by the GK effect, so the issue remains uncertain. Han (2008) just states that, in absence of the GK effect, his predicted f should be smaller at any age.

We conclude that the confirmation and refinement of Han (2008) model require more precise empirical f measurements in these and other globular clusters, that could even help constraining the model parameters, in particular the physically-important and poorly-known common envelope efficiency α_{CE} (see Han 2008, for a discussion).

7. Summary

We analyzed radial velocity variations for 51 hot HB/EHB stars in two Galactic globular clusters, in search for signatures of close binary systems. We also studied low-resolution spectra of program stars measuring temperature, surface gravity, helium abundance and mass. Our main results can be summarized as follows:

- In M 80 we confirm the anomalous behavior of spectroscopic masses found in NGC 6752 (Moni Bidin et al. 2007) for stars hotter than 23 000 K, although this result is less evident due to a smaller sample. Stars being fainter and/or redder show too high masses with respect to theoretical expectations, whereas their lower luminosities would suggest lower masses. In NGC 5986 the small number of EHB target observed prevents such an analysis.
- For the first time we observe a clear trend of helium abundance with temperature along the entire blue HB. These results confirm that helium depletion due to atmospheric diffusion reaches a maximum at about 15 000 K, then the helium abundance rises again with increasing temperature.

[5] The GK selection effect is an observational bias against EHB stars with a companion of G-K spectral type, because of the composite spectrum, or earlier, because of spectral dominance of the companion.

This behavior agrees qualitatively with expectations for the effects of diffusion at different temperatures along the HB. Somewhere at about 23 000 K the helium abundance could start to decrease again, but the observed pattern is hard to decipher. For these hot stars helium is depleted between a factor of 10 and 100, without a clear trend with temperature, nor a relation with the previously mentioned dichotomy on calculated masses.

- We detect one EHB close binary candidate per cluster. Their RV variations are quite small compared to typical sdB binary systems, but the probability of their being due to random errors is negligible. The candidate in M 80 is slightly cooler than typical EHB stars ($T_{\rm eff}$ = 18 100 K). None of them, nor any other EHB target, show the MgIb triplet as signature of a cool companion, at variance with the only other sdB close binary discovered to date in a globular cluster (Moni Bidin et al. 2008a). Therefore their companions are more likely compact objects such as white dwarfs, or very low-mass main sequence stars.
- The best estimate for the EHB close binary fraction in NGC 5986 is $f = 25\%$. This suggests that the fraction could be small, but no value lower than 70% can safely be excluded because of the small observed sample. Nevertheless, the probability of a very high binary fraction is low.
- In M 80 EHB close binaries with period shorter than 5 days are lacking with respect to what is observed among field sdB stars. The best estimate is $f_{P\leq5\ \rm days} = 12\%$, and within a 90% confidence level $f_{P\leq5\ \rm days} \leq 38\%$. The fraction is not very well determined, but even the lowest values found for field stars are very improbable and can be ruled out. Results fairly agree with the tiny $f = 4\%$ found in NGC 6752 (Moni Bidin et al. 2008a). M 80 is the second cluster for which this behavior is observed. This indicates that it is not just a peculiarity of NGC 6752 but it should be quite a common feature, posing important new constraints on models concerning sdB star formation.
- Our results agree with the existence of an f-age relation for sdB star populations, as proposed by Moni Bidin et al. (2008a) and theoretically modeled by Han (2008) in the framework of binary scenarios for their formation. Uncertainties in both predicted and observed values prevent their direct comparison. Nevertheless, we find that the f-age relation modeled by Han (2008) has some problem in reproducing the details of the observations. A refined set of model parameters could be needed, or the intervention of some other effect able to affect f and varying from cluster to cluster, like for instance dynamical interactions in dense environment.

The low binary fraction among globular cluster EHB stars is consistent with the typical (low) binary fraction among globular cluster stars. After all, the high binary fraction of sdB stars might not be a peculiarity related to their nature of hot He burning stars, but a simple consequence of the high binary fraction among field stars. If so, we still need to identify the cause of sdB star formation. Nevertheless, recent refined binary models can (at least qualitatively) account for the lack of *close* EHB systems in globular clusters, still retaining the hypothesis of a binary origin (Han 2008). Thus, the "binary scenario" cannot be ruled out by current observations, and we are still far from a full understanding of the complete picture.

Acknowledgements. We want to thank the staff at the La Silla Paranal Observatory for their support during our observations, and the referee for his comments and suggestions, that improved the paper. GP Acknowledge support by MIUR under the program PRIN2007 "Popolazioni Multiple in Ammassi GLobulari: Censimento, Caratterizzazione, Origine".

References

Allard, F., Wesemael, F., Fontaine, G., Bergeron, P., & Lamontagne, R. 1994, AJ, 107, 1565
Aznar Cuadrado, R., & Jeffery, C. S. 2001, A&A, 368, 994
Bedin, L. R., Piotto, G., Anderson, J., et al. 2004, ApJ, 605, L125
Behr, B. B. 2003, ApJS, 149, 67
Behr, B. B., Cohen, J. G., McCarthy, J. K., & Djorgovski, S. G. 1999, ApJ, 517, L135
Behr, B. B., Cohen, J. G., & McCarthy, J. K. 2000, ApJ, 531, L37
Bergeron, P., Saffer, R. A., & Liebert, J. 1992, ApJ, 394, 228
Brault, J. W., & White, O. R. 1971, A&A, 13, 169
Caloi, V. 1972, A&A, 20, 357
Catelan, M. 2005, in Resolved Stellar Populations, ASP Conf. Ser., in press [arXiv:astro-ph/0507464]
D'Antona, F., Bellazzini, M., Caloi, V., et al. 2005, ApJ, 631, 868
De Angeli, F., Piotto, G., Cassisi, S., et al. 2005, AJ, 130, 116
Denissenkov, P. A., & VandenBerg, D. A. 2003, ApJ, 598, 1246
Edelmann, H., Heber, U., Hagen, H.-J., et al. 2003, A&A, 400, 939
Edelmann, H., Heber, U., & Napiwotzki, R. 2006, Baltic Astron., 15, 103
Fabbian, D., Recio-Blanco, A., Gratton, R. G., & Piotto, G. 2005, A&A, 434, 235
Faulkner, J. 1966, ApJ, 144, 978
Ferguson, D. H., Green, R. F., & Liebert, J. 1984, ApJ, 287, 320
Flower, P. J. 1996, ApJ, 469, 355
Fontaine, G., & Chayer, P. 1997, in The Third Conference on Faint Blue Stars, ed. A. G. D. Philip, J. Liebert, R. Saffer, & D. S. Hayes, 169
Fontaine, G., Green, E. M., Chayer, P., et al. 2006, Baltic Astron., 15, 211
Glaspey, J. W., Demers, S., Moffat, A. F. J., & Shara, M. 1985, ApJ, 289, 326
Glaspey, J. W., Michaud, G., Moffat, A. F. J., & Demers, S. 1989, ApJ, 339, 926
Greenstein, J. L. 1971, in White Dwarfs, IAU Symp., 42, 46
Greggio, L., & Renzini, A. 1990, ApJ, 364, 35
Grundahl, F., Catelan, M., Landsman, W. B., Stetson, P. B., & Andersen, M. I. 1999, ApJ, 524, 242
Hamuy, M., Suntzeff, N. B., Heathcote, S. R., et al. 1994, PASP, 106, 566
Han, Z. 2008, A&A, 484, L31
Han, Z., Podsiadlowski, P., Maxted, P. F. L., Marsh, T. R., & Ivanova, N. 2002, MNRAS, 336, 449
Han, Z., Podsiadlowski, P., Maxted, P. F. L., & Marsh, T. R. 2003, MNRAS, 341, 669
Han, Z., Podsiadlowski, P., & Lynas-Gray, A. E. 2007, MNRAS, 380, 1098
Harris, W. E. 1996, AJ, 112, 1487
Heber, U. 1986, A&A, 155, 33
Heber, U., Moehler, S., Napiwotzki, R., Thejll, P., & Green, E. M. 2002, A&A, 383, 938
Hirsch, H. A., Heber, U., & O'Toole, S. J. 2008, in ASP Conf. Ser., 392, 131
Horne, K. 1986, PASP, 98, 609
Hoyle, F., & Schwarzschild, M. 1955, ApJS, 2, 1
Kurucz, R. 1993, ATLAS9 Stellar Atmosphere Programs and 2 km s grid. Kurucz CD-ROM No. 13. Cambridge, Mass.: Smithsonian Astrophysical Observatory
Lee, Y., Joo, S., Han, S., et al. 2005, ApJ, 621, L57
Lisker, T., Heber, U., Napiwotzki, R., et al. 2005, A&A, 430, 223
Maxted, P. F. L., Heber, U., Marsh, T. R., & North, R. C. 2001, MNRAS, 326, 1391
Menzies, J. W., & Marang, F. 1986, in Instrumentation and Research Programmes for Small Telescopes, IAU Symp., 118, 305
Michaud, G., & Charland, Y. 1986, ApJ, 311, 326
Michaud, G., Vauclair, G., & Vauclair, S. 1983, ApJ, 267, 256
Michaud, G., Bergeron, P., Wesemael, F., & Heber, U. 1989, ApJ, 338, 417
Michaud, G., Richer, J., & Richard, O. 2008, ApJ, 675, 1223
Miocchi, P. 2007, MNRAS, 381, 103
Moehler, S. 2001, PASP, 113, 1162
Moehler, S., & Sweigart, A. V. 2006, A&A, 455, 943
Moehler, S., Heber, U., & de Boer, K. S. 1995, A&A, 294, 65
Moehler, S., Sweigart, A. V., & Catelan, M. 1999, A&A, 351, 519
Moehler, S., Sweigart, A. V., Landsman, W. B., & Heber, U. 2000, A&A, 360, 120
Moehler, S., Sweigart, A. V., Landsman, W. B., & Dreizler, S. 2002, A&A, 395, 37
Moehler, S., Landsman, W. B., Sweigart, A. V., & Grundahl, F. 2003, A&A, 405, 135
Momany, Y., Piotto, G., Recio-Blanco, A., et al. 2002, ApJ, 576, L65
Momany, Y., Cassisi, S., Piotto, G., et al. 2003, A&A, 407, 303

Momany, Y., Bedin, L. R., Cassisi, S., et al. 2004, A&A, 420, 605
Moni Bidin, C., Moehler, S., Piotto, G., et al. 2006a [arXiv:astro-ph/0606035]
Moni Bidin, C., Moehler, S., Piotto, G., et al. 2006b, A&A, 451, 499
Moni Bidin, C., Moehler, S., Piotto, G., Momany, Y., & Recio-Blanco, A. 2007, A&A, 474, 505
Moni Bidin, C., Catelan, M., & Altmann, M. 2008a, A&A, 480, L1
Moni Bidin, C., Catelan, M., Villanova, S., et al. 2008b, in ASP Conf. Ser., 392, 27
Morales-Rueda, L., Maxted, P. F. L., Marsh, T. R., North, R. C., & Heber, U. 2003, MNRAS, 338, 752
Morales-Rueda, L., Maxted, P. F. L., Marsh, T. R., Kilkenny, D., & O'Donoghue, D. 2006, Baltic Astron., 15, 187
Moran, C., Maxted, P., Marsh, T. R., Saffer, R. A., & Livio, M. 1999, MNRAS, 304, 535
Munari, U., Sordo, R., Castelli, F., & Zwitter, T. 2005, A&A, 442, 1127
Napiwotzki, R., Green, P. J., & Saffer, R. A. 1999, ApJ, 517, 399
Napiwotzki, R., Karl, C. A., Lisker, T., et al. 2004, Ap&SS, 291, 321
Norris, J. E. 2004, ApJ, 612, L25
O'Toole, S. J. 2008, in ASP Conf. Ser., 392, 67
Pace, G., Recio-Blanco, A., Piotto, G., & Momany, Y. 2006, A&A, 452, 493
Piotto, G., King, I. R., Djorgovski, S. G., et al. 2002, A&A, 391, 945
Piotto, G., Villanova, S., Bedin, L. R., et al. 2005, ApJ, 621, 777
Piotto, G., Bedin, L. R., Anderson, J., et al. 2007, ApJ, 661, L53
Recio-Blanco, A., Piotto, G., Aparicio, A., & Renzini, A. 2002, A&A, 572, L71
Reed, M. D., & Stiening, R. 2004, PASP, 116, 506
Rich, R. M., Sosin, C., Djorgovski, S. G., et al. 1997, ApJ, 484, L25
Saffer, R. A., Bergeron, P., Koester, D., & Liebert, J. 1994, ApJ, 432, 351
Saffer, R. A., Livio, M., & Yungelson, L. R. 1998, ApJ, 502, 394
Sandage, A., & Wildey, R. 1967, ApJ, 150, 469
Schwarzschild, M., & Härm, R. 1962, ApJ, 136, 158
Silvotti, R., Schuh, S., Janulis, R., et al. 2007, Nature, 449, 189
Soker, N. 1998, AJ, 116, 1308
Ströer, A., Heber, U., Lisker, T., Napiwotzki, R., & Dreizler, S. 2005, in ASP Conf. Ser., 334, 309
Suda, T., Tsujimoto, T., Shigeyama, T., & Fujimoto, M. Y. 2007, ApJ, 671, L129
Sweigart, A. 2000, Mixing and Diffusion in Stars: Theoretical Predictions and Observational Constraints, 24th meeting of the IAU, Joint Discussion 5
Sweigart, A. V. 1997, ApJ, 474, L23
Sweigart, A. V., & Mengel, J. G. 1979, ApJ, 229, 624
Tonry, J., & Davis, M. 1979, AJ, 84, 1511
Tüg, H. 1977, The Messenger, 11, 7
Ulla, A., & Thejll, P. 1998, A&AS, 132, 1
Unglaub, K. 2008, A&A, 486, 923
Unglaub, K., & Bues, I. 1998, A&A, 338, 75
van den Bergh, S. 1967, AJ, 72, 70
Vink, J. S., & Cassisi, S. 2002, A&A, 392, 553
von Rudloff, I. R., Vandenberg, D. A., & Hartwick, F. D. A. 1988, ApJ, 324, 840
Vučković, M., Aerts, C., Østensen, R., et al. 2007, A&A, 471, 605
Williams, T., McGraw, J. T., Mason, P. A., & Grashuis, R. 2001, PASP, 113, 944